

Screen-printed phosphor coatings for white LED emission

Julien Burgin · Véronique Jubera · Hélène Debéda ·
Benoit Glorieux · Alain Garcia · Claude Lucat

Received: 26 July 2010/Accepted: 9 November 2010/Published online: 30 November 2010
© Springer Science+Business Media, LLC 2010

Abstract We demonstrate the possibilities offered by the screen-printing technique to create thick layers of rare earth doped phosphors on glass slides for light-emitting diodes (LEDs). Using commercial LEDs, the effect of the layer thickness and phosphor concentration on luminescence emission and chromaticity are investigated. The advantages offered by screen-printed multi-phosphors systems are also revealed through a feasibility study permitting to tune the chromatic coordinate of the global light emission by modifying the phosphors characteristics independently.

Introduction

One of the major achievements in semiconductor science during the past decade, from both a fundamental and applied point of view, has been the development of nitride-based light-emitting diodes (LEDs) [1]. In the field of lighting, which is a very hot topic in greenhouse effect gases emission reduction, it offers the possibility to produce white LEDs using additive mixing with several colored diodes or phosphor coatings [2, 3]. In the latter case, yttrium aluminum

garnet activated with trivalent cerium, $\text{Y}_3\text{Al}_5\text{O}_{12}:\text{Ce}^{3+}$ (YAG:Ce), has proven to be a very efficient phosphor when coupled with a blue diode to generate white light by mixing the incident blue diode light and the fluorescent yellow emission. For lighting applications, efficiency, stability, and chromaticity are crucial parameters. A 5500 K black-body radiation is attainable with tungsten filaments but remains quite difficult for white LEDs [3, 4]. In this context, several aspects have been investigated: global LED efficiency and chromaticity tunability. The efficiency is improved by changing the LED chip design and its coating [5–7]. The optimization of the chromaticity coordinates is generally addressed by using new rare earth doping with the YAG matrix [8, 9] or substituted YAG matrix [10]. Another promising route is the use of new families of phosphors [11–13], new types of luminescent materials such as silicon nanoparticles [14], semi-conductor nano-crystals [15], or organic phosphors [16].

Here we suggest a route to tune the chromaticity of white LEDs based on coupling blue or UV diodes with phosphor coatings and utilizing a low cost screen-printing technique. Using this technique, we deposit a well defined and homogeneous thick film using an organic paste blended with a phosphor powder. This technique, mainly used in microelectronics for interconnections and packaging purposes [17], has been extended to development of passive components such as sensors and micro-electro-mechanical systems (MEMS) [18]. Screen-printing is very attractive for LEDs applications, because the coatings can be structured by alternating or stacking phosphor layers of different composition, width, and thickness. The thickness can vary from few μm to 100 μm , with a minimum line width of 100 μm . This microstructuration offers the opportunity to tune the deposited layers and then, the emitted light spectral properties. Moreover, this thick-film

J. Burgin · V. Jubera · B. Glorieux · A. Garcia
CNRS, Université de Bordeaux, ICMCB,
87 av. Dr. A. Schweitzer, 33608 Pessac, France

H. Debéda · C. Lucat
Université de Bordeaux, IMS, 351 Cours de la Libération,
33405 Talence Cedex, France

Present Address:
J. Burgin (✉)
Université de Bordeaux, CPMOH, 351 cours de la
Libération, 33405 Talence Cedex, France
e-mail: j.burgin@cpmoh.u-bordeaux1.fr

technology is fully compatible with industrial processes and the “phosphor-on-top” design which presents a more favorable global yield compared to conventional packages [6, 7].

In this work, we deposited phosphors on substrates and characterized the coatings. We studied their fluorescent properties versus their thickness and concentration, especially for the YAG:Ce phosphor. In a configuration combining a commercial InGaN diode and screen-printed layers, we studied the emitted light and tuned its chromaticity, taking advantage of the micro-structuration possibilities offered by screen-printing.

Experiment

We synthesized yellow emitting $\text{Y}_3\text{Al}_5\text{O}_{12}:\text{Ce}^{3+}$ (YAG:Ce) and red emitting $\text{Li}_6\text{Y}(\text{BO}_3)_3:\text{Eu}^{3+}$ (LYB:Eu) phosphors using a co-precipitation method [19]. Preparation of YAG:Ce with a composition of $3(1-x)/2 \text{ Y}_2\text{O}_3:5/2 \text{ Al}_2\text{O}_3:3 \times \text{CeO}_2$ ($x\%$ doping) is achieved by mixing and milling Y_2O_3 (Rhodia, 99.999%), Al_2O_3 (Acros, 99.99%), and CeO_2 (Reacton, 99.99%) powders. Then, in order to obtain a homogeneous distribution of the constituents, 4 mg of the mixture is added to 10 mL of nitric acid (Prolab 68% HNO_3) and heated to approximately 50 °C until the solvent evaporates. The white brown sticky substance obtained is then milled and heated for 6 h at 450 °C (in an argon atmosphere) prior to a final firing of 10 h at 1400 °C under a reducing atmosphere (90% Ar, 10% H_2), with intermediate grinding. The products are then manually milled with an agate mortar followed by 1 h of planetary ball grinding. To synthesize LYB:Eu, stoichiometric amounts of Li_2CO_3 (Merck, >99%), Y_2O_3 (Rhodia, 99.999%), H_3BO_3 (Merck, 99.8%), and Eu_2O_3 (Reacton, 99.99%) are mixed in nitric acid solution and evaporated at 50 °C to dryness before milling. Samples are first heated during 2 h at 450 °C, then at 750 °C and finally fired 14 h at 900 °C under O_2 atmosphere, with intermediate grinding [20].

The final products are characterized by X-ray diffraction (XRD) using a Bragg-Bentano Philips PW1820 diffractometer working with the CuK_α radiation and a backward monochromator and they are found to be pure. Emission and excitation spectra are collected using a 450 W Xenon lamp with and Jobin-Yvon SPEX spectrofluorimeter with two monochromators and a R928P Hamamatsu photomultiplier in the UV-visible range. This setup is conventionally used to measure scattered fluorescence emitted by phosphors layers or using the second monochromator as a simple analyzer when the phosphor layer is coupled with a LED chip. The diode chips used are commercial InGaN LEDs emitting at 470 nm or 393 nm and will be called blue LED or UV LED, respectively, in the following text.

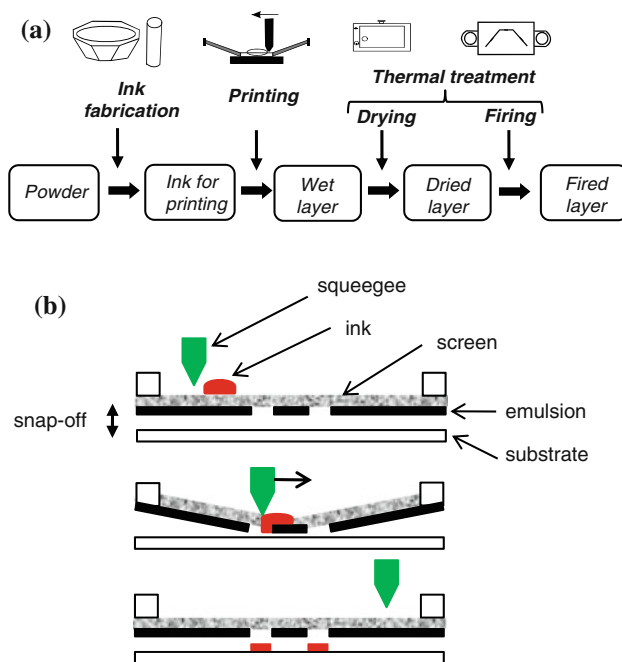


Fig. 1 Illustration of the thick film process (a) and the screen-printing technique (b)

The screen-printing process is performed with a Schmidt setup shown in Fig. 1. This process requires specific inks, made of powders and organic binder mixed together, to be transferred onto the substrate through open areas of meshes of the patterned screen by a squeegee. The deposited film is then dried and, in case of glass-based cermet pastes, fired to achieve sintering and adherence of the thick film on the substrate (Fig. 1a).

Results and discussion

Screen-printed phosphor layers

A polymer ink, based on a mixture of epoxy and phosphor powder (few μm diameter grains) is prepared for the phosphor layer screen-printing. This polymer-based paste has two advantages for our application: its thermal treatment compatibility (30 min at 120 °C) with many substrates and the absence of optical contaminants. Pastes with different powder concentrations (from 8 to 30% in volume) were fabricated in order to study the influence of phosphor dispersion on luminescence. The deposition of 250 μm width tracks can be obtained using a 325 mesh screen. Different layer thicknesses are deposited (from 10 to 80 μm once dried) to find the optimal thickness regarding the luminescence properties. The final thickness mainly depends on the screen-substrate distance (the snap-off) and the emulsion thickness on the screen (Fig. 1b). The layers

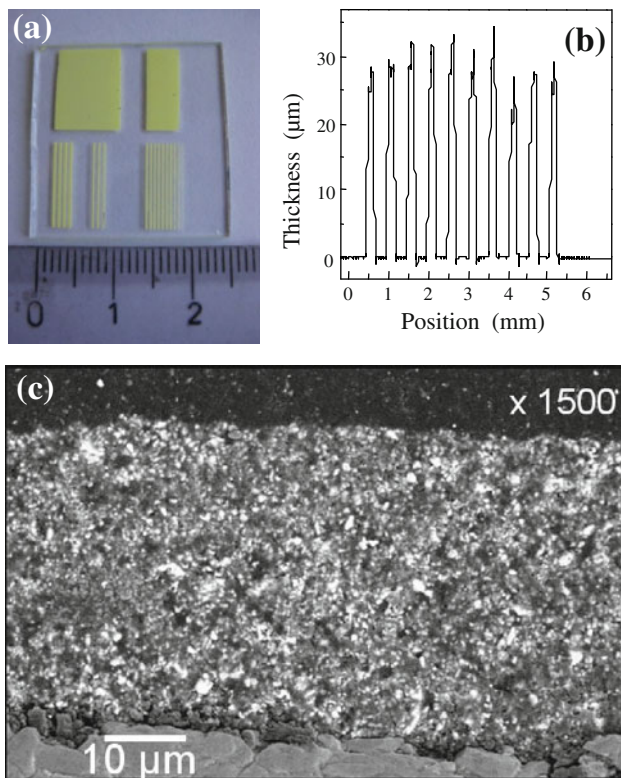


Fig. 2 **a** Photography of a screen-printed YAG:Ce layer on a glass substrate. **b** Measured profile of screen-printed stripes. **c** SEM picture of a micro-section of a YAG:Ce (41 vol.%) screen-printed layer on alumina

are deposited on alumina or on glass substrate (microscope glass slide) when testing the optical properties (Fig. 2a). After deposition, the films are dried 30 min at 120 °C for solvent evaporation and epoxy polymerization (Fig. 1a).

The layers are characterized with an optical profilometer (Altisurf 500) to measure the layer thicknesses and widths (Fig. 2b). Screen-printing enables us to make stripes (around 250 μm) with good reproducibility and clean edges. In our case, slight differences in thicknesses are attributed to variance in the glass substrate flatness. The volume reduction of the screen-printed layers during the drying because of solvent evaporation is also measured with the Altisurf 500. The real volume concentration of phosphors in the final layer is then deduced. After drying, a paste containing 8 vol.% of phosphor powder becomes an epoxy layer loaded with 28 vol.% of phosphors.

Dispersion of the phosphors in the epoxy is observed using a scanning electron microscope (JEOL 820 operating at 10 kV). A micro-section of a 40 μm thick layer of YAG:Ce deposited on alumina shows that the phosphor grains have a size around 1 μ, are well distributed, and do not aggregate during this process (Fig. 2c).

After the demonstration of phosphor layers screen-printing in standard conditions and the study of their

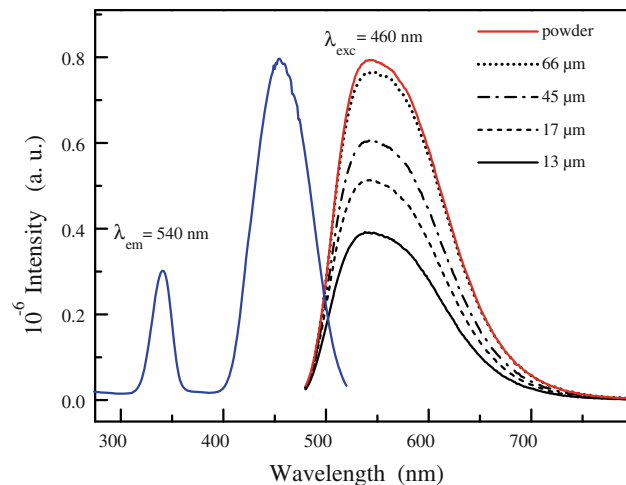


Fig. 3 Excitation ($\lambda_{\text{em}} = 540 \text{ nm}$) and emission ($\lambda_{\text{exc}} = 460 \text{ nm}$) spectra of YAG:Ce phosphor powder compared with emission spectra of YAG:Ce screen-printed layers of different thicknesses (phosphor dispersion: 46 vol.%)

structural properties, we will now focus on their optical properties.

Thickness and concentration effect

The luminescence spectra of YAG:Ce layers is measured and compared with the YAG:Ce powder for different layer thicknesses deposited on glass with a paste leading to 46 vol.% phosphor films (Fig. 3). Due to the $5d$ - $4f$ emission of Ce^{3+} , two absorption bands at 340 nm and 460 nm and a broad emission band around 540 nm are, respectively, obtained for the excitation spectrum ($\lambda_{\text{em}} = 540 \text{ nm}$) and the emission spectrum ($\lambda_{\text{exc}} = 460 \text{ nm}$ or 340 nm) for the raw powder [21]. This latter band is constituted by the radiative de-excitation from the lowest $5d$ energy level down to the two $^2\text{F}_{7/2}$ and $^2\text{F}_{5/2}$ levels. Emission spectra shapes are found to be the same in the screen-printed samples. Even more, for a sufficient layer thickness (66 μm) the same intensity level as the raw powder is closely reached. This can be interpreted in terms of penetration depth. Since raw powder is quite compact the collected scattered luminescence only comes from a thin surface layer, after which the incident light is fully absorbed or scattered. Though it is difficult to estimate the penetration depth in a granular phosphor medium, one may assume it is about few microns. In the case of screen-printed layers, the phosphor grains are spaced by transparent epoxy (Fig. 2c) and thus, more excitation light reaches the substrate without being scattered or absorbed. This consequently reduces the luminescence intensity compared to the raw powder when it is measured in the same conditions as the excitation level of the phosphor is effectively lower. In these experiments, we use a glass

substrate and a black sample holder in order to limit multiple reflection phenomena. By increasing the layer thickness the luminescence intensity increases up to a threshold value, which is identical to the raw powder case (Fig. 3).

To address this feature, similar studies are performed for several phosphor concentrations. Figure 4a shows the summary of this study: the integrated luminescence intensity (normalized to the raw powder) for an excitation at $\lambda_{\text{exc}} = 460 \text{ nm}$ is plotted versus the layer thickness for five different phosphor volume concentrations. When the concentration increases, the raw powder luminescence intensity is reached for smaller thicknesses. This is interpreted by considering the penetration depth previously mentioned: this penetration depth will be shorter for a high concentrated coating since the excitation light will interact with the same number of grains in a shorter path than for a less concentrated coating. This penetration depth is directly related to an accessible parameter, the characteristic length, L , extracted from the data by fitting with the following function:

$$I_x = A(1 - e^{-\frac{x}{L}}) \quad (1)$$

where A is the integrated intensity of the raw powder (normalized to 1 in this study) and x the layer thickness. This simple expression represents the luminescence intensity coming out of the front side of the sample. It can be derived from a Kubelka–Munk model (KM) taking fluorescence into account when the luminescence re-absorption is neglected [22]. The data in Fig. 4a are well fit by Eq. 1. The inverse of the characteristic length, which is the relevant parameter, is plotted as a function of the concentration (Fig. 4b). This figure shows that this parameter is non-linear with the concentration: the characteristic length drastically decreases with the phosphor concentration, where the KM model that predicts a linear behavior. This observation shows that the scattering and absorption process are more complex in our system than what is depicted by the KM model where the scattering does not depend on the phosphor concentration.

We observe that the scattered fluorescent light of screen-printed layers depends on their phosphor concentration and thickness, and present similar properties to the phosphor powder. We will now address their properties in transmission when coupled with diode chips.

LEDs and YAG:Ce screen-printed layers

To illustrate the possibilities offered by this thick-film process, experiments using commercial diodes as excitation sources were performed. The glass, covered by the thick layer, is fixed on the top of the diode as depicted in Fig. 5a. We first measure the emitted spectra using a 470 nm InGaN diode for several input currents and

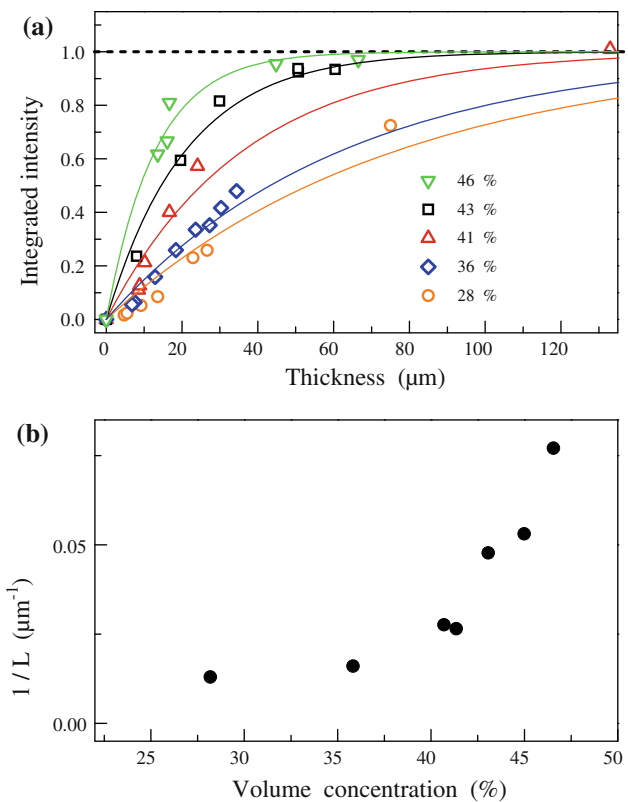


Fig. 4 **a** Integrated photoluminescence intensity for several screen-printed YAG:Ce inks as a function of the layer thickness (dots). Fits using Eq. 1, compared with the full powder case (horizontal dotted line), **b** inverse of the characteristic length L , obtained by fitting data of **a** with Eq. 1, plotted as a function of the phosphor volume concentration in the layer

YAG:Ce layers of several thicknesses. Figure 6a shows emitted spectra of a 470 nm InGaN diode coupled with a 30 μm thick YAG:Ce layer for several input currents. The yellow luminescence is present in each case but its intensity depends on the input current. Figure 7 shows that the CIE xy coordinates [23, 24] of the transmitted spectra weakly depend on the input current (Table 1; Fig. 7 inset): they follow the intrinsic spectral drift of the diode with current. Figure 6b shows the effect of phosphor thickness for a given current. As expected, it shows that an increase in the YAG:Ce thickness increases the yellow luminescence intensity.

The CIE coordinates of the blue LED chip alone (0.125, 0.09), the YAG:Ce layer alone (0.41, 0.55) (fluorescence experiment with a Xe lamp) and the transmitted light when they are associated, are compared in Table 1. The CIE coordinates strongly depend on the layer thickness, as shown by the empty circles in Fig. 7. A typical thickness of 30 μm for a 40 vol.% concentrated layer allows us to get close to white light (1/3, 1/3). The CIE coordinates reached (0.265, 0.349) are indeed close to the best characteristics one can get since the resulting CIE coordinates are between

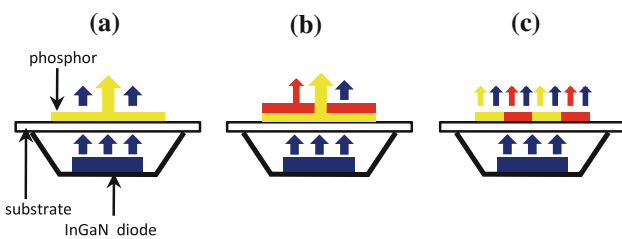


Fig. 5 Drawing of the combination of commercial LED with several screen-printed layers mimicking “phosphor-on-top” design [5, 6], **a** diode and YAG:Ce layer, **b** diode and superposed YAG:Ce and LYB:Eu layers, **c** diode and striped layers (YAG:Ce and LYB:Eu)

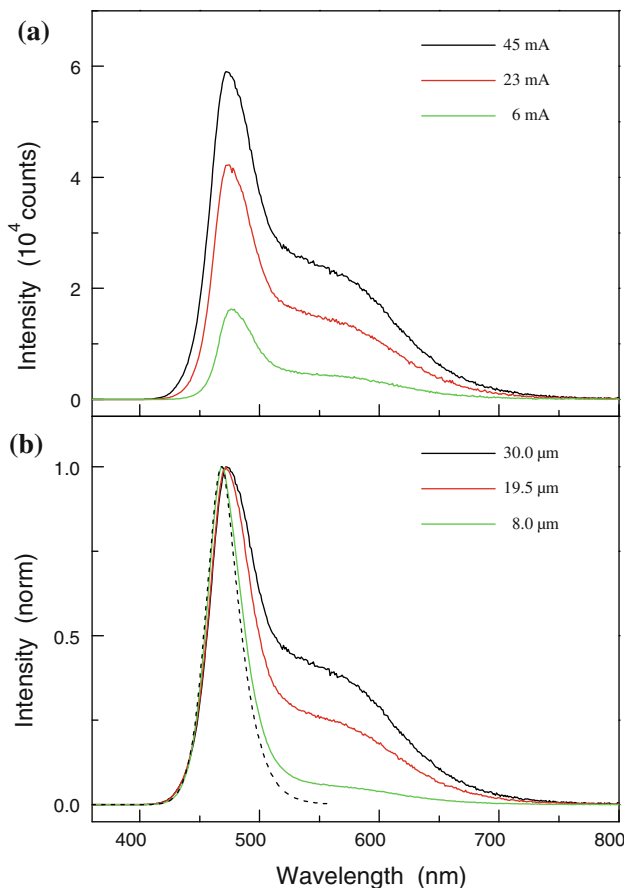


Fig. 6 **a** Emission spectra of a blue LED coupled with a 30 μm thick screen-printed YAG:Ce layer for several input currents, **b** normalized emission spectra of a blue LED working at 45 mA alone (dots) or coupled with YAG:Ce layers of different thicknesses

the blue LED and the YAG:Ce dots (Table 1; Fig. 7). These kinds of packages are already commercially available with equivalent CIE coordinates, however, their bluish hue is not optimized for domestic lighting.

LEDs and multi-phosphors screen-printed layers

A way to get closer to white light is to include another phosphor. The versatility of screen-printing allows us to print

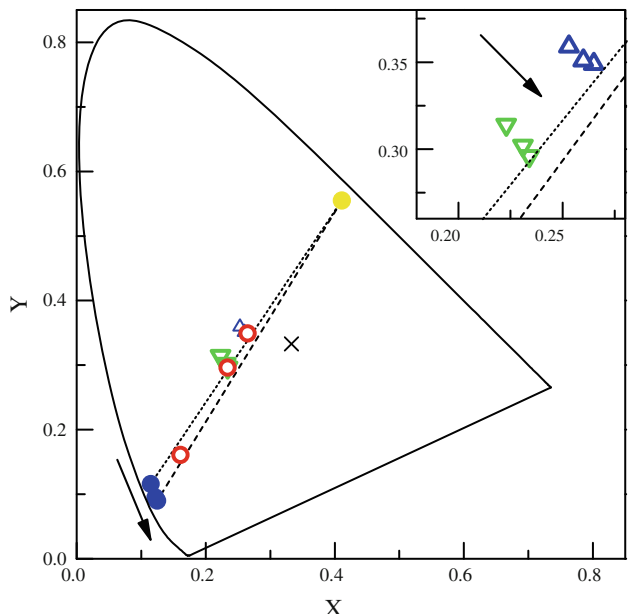


Fig. 7 CIE chromatic coordinates of a blue LED (full circles) for several currents (6, 23 and 45 mA, increasing current along the arrow), screen-printed phosphor layers alone (full light gray/yellow circle) and their association with the diode for several YAG:Ce thicknesses (empty circles) and current (empty triangles). The dashed and dotted lines link CIE coordinates of LED and phosphor alone to show available coordinates. The inset is a zoom showing the effect of input current (increasing current along the arrow) (Color figure online)

Table 1 CIE coordinates of the YAG:Ce emission and blue LED when they are alone or associated for several input currents

Input current	CIE coordinates for several LED input current		
	6 mA	23 mA	45 mA
Blue LED chip alone	(0.115, 0.116)	(0.122, 0.095)	(0.125, 0.09)
LED + 8 μm layer	–	–	(0.161, 0.161)
LED + 19 μm layer	(0.223, 0.314)	(0.231, 0.302)	(0.234, 0.296)
LED + 30 μm layer	(0.253, 0.359)	(0.260, 0.351)	(0.265, 0.349)
YAG:Ce alone	(0.41, 0.55)		

The data correspond to Fig. 7

several phosphors in multiple ways. Successive phosphor layers (Fig. 5b) or thin stripes can be printed without mixing phosphors (Fig. 5c) and coupled with diodes. These opportunities are investigated using the LYB:Eu as a second phosphor, which presents several red emission peaks. This phosphor is chosen because its narrow-band emission spectrum makes it easily recognizable when superimposed with the broad band of the first phosphor (YAG:Ce). Its CIE coordinates are (0.65, 0.35) for the raw powder and screen-printed samples when excited at $\lambda_{\text{exc}} = 393 \text{ nm}$.

We prepare inks resulting in 36 vol.% YAG:Ce and 34 vol.% LYB:Eu dried layers, in order to get similar intensities for both phosphors layers. The layers are

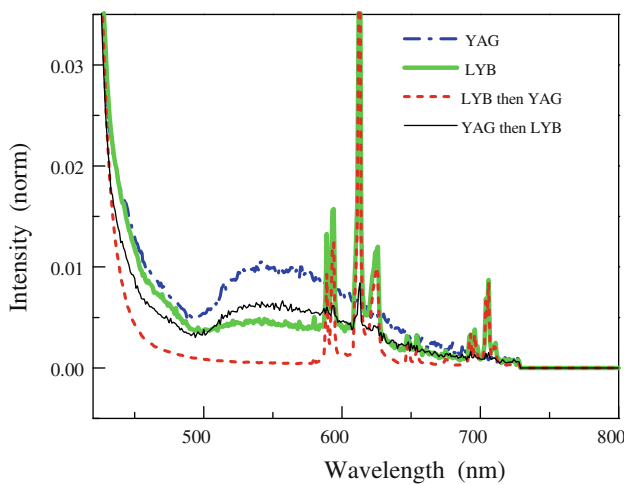


Fig. 8 Emission spectra of a UV LED coupled with a screen-printed layer for a 50 mA input current. The *dot-dashed blue* and *dashed red* lines are obtained for a single layer of YAG:Ce and LYB:Eu, respectively. The *full lines* for a YAG:Ce and LYB:Eu layers (YAG:Ce then LYB:Eu for the thin black, LYB:Eu then YAG:Ce for the thick green) (Color figure online)

screen-printed and dried successively. We first investigate the successive layer case with 75 μm thick samples (Fig. 5b). We measured emission spectra at 393 nm for YAG:Ce and LYB:Eu screen-printed layers in the classic fluorescence setup (Xe lamp) and measured the transmitted light through a layer coupled with a UV LED working at 50 mA. The latter spectra are shown in Fig. 8. The dashed red plot shows emission spectra of the LYB:Eu layer in transmission, identified by the two series of peaks at 600 nm and 700 nm due to the $^5\text{D}_0 - ^7\text{F}_j$ transitions [20]. The dotted yellow curve is obtained with a single YAG:Ce layer, showing a broad 540 nm emission band. Note here that these emissions are quite weak compared to the UV LED spectrum because of the weak absorption coefficient of the YAG:Ce in this spectral region and the low quantum yield of LYB:Eu. This configuration is an illustration of a multi-phosphor design and does not correspond to a reasonable combination for a final device. We calculate the CIE coordinates of these spectra and compare them with the diode alone or the layers excited by the Xe lamp (Table 2; Fig. 9 full dots). The layers coupled with the diodes fall between the diode and the layers alone (Table 2; Fig. 9 empty circles). They are found to be not that close to the UV LED coordinates due to the weak contribution of the UV-blue part of the light (essentially from the UV LED) to the CIE coordinates. We also perform measurements for these two screen-printed layers together (in both orders) coupled with the UV LED in similar conditions (Fig. 8). We observe that the sharp LYB:Eu peaks are stronger when the UV light first reaches the LYB:Eu layer but, however, this weakens the YAG:Ce yellow emission. A similar behavior is found when the UV light reaches the

Table 2 CIE coordinates of YAG:Ce, LYB:Eu emission and UV LED when they are alone or associated

	Phosphors alone	+ UV LED
UV LED chip alone	—	(0.171, 0.012)
YAG:Ce	(0.41, 0.55)	(0.240, 0.173)
LYB:Eu	(0.645, 0.349)	(0.227, 0.058)
LED then LYB:Eu then YAG:Ce		(0.239, 0.119)
LED then YAG:Ce then LYB:Eu		(0.227, 0.137)
LED + striped layer no 1		(0.221, 0.08)
LED + striped layer no 2		(0.236, 0.112)
LED + striped layer no 3		(0.243, 0.147)

The data correspond to Fig. 9

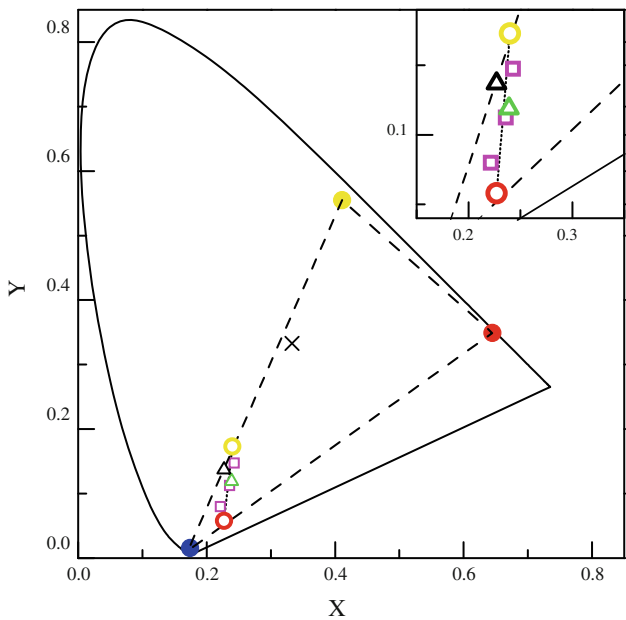


Fig. 9 CIE chromatic coordinates of YAG:Ce (yellow/light gray full circle) and LYB (red/light gray full circle) layers and a UV LED single (blue/dark gray full circle) or coupled with LYB and YAG:Ce layers : YAG:Ce only (empty yellow/light gray circle), LYB only (empty red/light gray circle), LYB then YAG:Ce (green/light gray triangle) and YAG:Ce then LYB (black triangle). The magenta empty squares represent the coordinates of YAG:Ce and LYB:Eu stripes of several thicknesses. The inset is a zoom (Color figure online)

YAG:Ce first, but results in a very weak LYB:Eu emission. In terms of CIE coordinates, when the LYB:Eu is first excited, the coordinates are close to the averaged single layer coordinates while when the YAG:Ce is excited first, the coordinates remain on the LED-YAG:Ce dashed line (Table 2; Fig. 9 triangles). This is due to the strong absorption of the YAG:Ce layer that does not let enough remaining UV to efficiently excite the LYB:Eu layer. This behavior is difficult to control since both layers are coupled: every modification of the first layer thickness or the input current affects the fluorescence emission of both phosphors and the resulting package chromaticity.

To get rid of this problem, samples with alternating stripes of YAG:Ce and LYB:Eu are screen-printed. The choice of their relative thickness allows us to tune the CIE coordinates between a pure YAG:Ce or LYB:Eu chromaticity without internal coupling (Table 2). The inset of Fig. 9 (squares) shows the coordinates of three different striped samples (sample 1: 75 µm LYB:Eu and 50 µm YAG:Ce, sample 2: 75 µm for both phosphors, sample 3: 75 µm LYB:Eu and 100 µm YAG:Ce). Finally, we can tune the chromaticity of the emitted light by changing phosphors independently.

This example shows up that a good LED phosphor deposition design is very important for chromaticity tuning and shows that screen printing, which allows the deposition of successive or striped layers, is an adapted technique for this important task.

Conclusion

We studied the fluorescence of screen-printed layers of several thicknesses and concentrations by spectrofluorimetry and their colorimetric coordinates when coupled with commercial InGaN LEDs. The advantages of screen-printing associated with commercial LEDs are shown. The possibilities offered by screen-printing with multi-phosphors are demonstrated using two phosphors and the tunability of the chromaticity of the total emitted light is illustrated using striped layers. This design allowed us to get rid of the re-absorption problems affecting the global chromaticity. This study opens up many possibilities for applications using the deposition of three-phosphor thick films (red, green, blue) on a carefully selected diode which emission is well absorbed by all phosphors. The screen-printing technique offers new possibilities for the design and engineering of complex phosphor layers on flat substrates. The use of this technique in practical application will depend on further characterization of the screen-printed layers, including thermostability, color rendering index, and luminous efficiency measurements of appropriated packages.

Acknowledgements The authors thank the Groupement d'Interet Scientifique Advanced Materials in Aquitaine (LasINOF) and the Region Aquitaine for financial support.

References

- Nakamura S, Pearton S, Fasol G (2000) The blue laser diode. The complete story. Springer, Heidelberg
- Zukauskas A, Shur MS, Gaska R (2001) Mater Res Sci Bull 26:764
- Hoppe HA (2009) Angew Int Ed 48:3572
- Schlotter P, Baur J, Hielscher Ch, Kunzer M, Obloh H, Schmidt R, Schneider J (1999) Mater Sci Eng B 59:390
- Allen SC, Steckl AJ (2008) Appl Phys Lett 92:143309
- Luo H, Kim JK, Schubert EF, Cho J, Sone C, Park Y (2005) Appl Phys Lett 86:243505
- Luo H, Kim JK, Xi YA, Schubert EF, Cho J, Sone C, Park Y (2006) Appl Phys Lett 89:041125
- Wang W, Tang J, Teng Hsu S, Wang J, Sullivan BP (2008) Chem Phys Lett 457:103
- Yang SH, Lu CY (2007) J Electrochem Soc 154:397
- Janga HS, Ima WB, Lee DC, Jeona DY, Kim SS (2007) J Lumin 126:371
- Park JK, Choi KJ, Kim KN, Kim CH (2005) Appl Phys Lett 87:031108
- Im WB, Kim YI, Fellows N, Masui H, Hirata G, DenBaars S, Seshadri R (2008) Appl Phys Lett 93:091905
- Yang H, Liu Y, Ye S, Qiu J (2008) Chem Phys Lett 451:218
- Sato K, Kishimoto N, Hirakuri K (2007) J Appl Phys 102:104305
- Anikeeva P, Halpert J, Bawendi M, Bulovic V (2009) Nano Lett 9:2532
- Park S, Kwon JE, Kim SH, Seo J, Chung K, Park SY, Jang DU, Medina BM, Gierschner J, Park SY (2009) J Am Chem Soc 131:14043
- Haskard M, Pitt K (1997) Thick film technology and applications. Electrochemical Publications, Isle of Man
- Lucat C, Ginet P, Ménil F (2007) J Microelectron Electron Packag 4:86
- Pan Y, Wu M, Su Q (2004) Mater Sci Eng B 106:251
- Jubera V, Chaminade JP, Garcia A, Guillen F, Fouassier C (2003) J Lumin 101:1
- Blasse G, Bril A (1967) J Chem Phys 47:5139
- Allen E (1964) J Opt Soc Am 54:506
- CIE (1931) Commission Internationale de l'Eclairage proceedings. Cambridge University Press, Cambridge
- Smith T, Guild J (1931) Trans Opt Soc 33:73